

Nano- and Microstructuring of Materials' Surfaces Using Femtosecond Laser Pulses

A. I. Gavrilov^a, D. V. Golovin^b, A. M. Emelyanenko^a, D. A. Zayarny^b, A. A. Ionin^b,
S. I. Kudryashov^{b, c}, S. V. Makarov^b, P. N. Saltuganov^{b, d}, and L. B. Boinovich^a

^a*Frumkin Institute of Physical Chemistry and Electrochemistry, Russian Academy of Sciences, Moscow, 117071 Russia*

^b*Lebedev Physical Institute, Russian Academy of Sciences, Moscow, 119991 Russia*

^c*National Research Nuclear University, Moscow Engineering Physics Institute (MEPhI), Moscow, 115409 Russia*

^d*Moscow Institute of Physics and Technology (State University), Dolgoprudny, Moscow oblast, 141700 Russia*

e-mail: masker19@list.ru

Abstract—Multimodal nano- and microscale surface textures are produced by scanning the surfaces of various structural materials using IR femtosecond laser radiation. The topographies of the modified surfaces and their wettabilities upon hydrophobization are studied.

DOI: 10.3103/S1062873816040122

INTRODUCTION

Multiscale nano- and microscaled surface textures substantially modify the physical and physicochemical properties of materials [1–4]. In many applications, it is the multimodal texture that is critical [4].

The quickest and least expensive method for manufacturing such textures is the laser ablation scanning (milling) of surfaces [1]. Ultra-short, femto-, and sub-picosecond pulse lasers, whose mechanisms of laser ablation have been thoroughly studied [5, 6], are a universal laser source for the laser texturing of diverse materials, from metals to dielectrics. Nevertheless, the multiscale nano- and microtexturing of some materials requires careful selection of the laser processing conditions within an enormous range of such experimental parameters as wavelength, duration, energy, ultra-short pulse repetition frequency, focusing, and surface scanning rate. Optimum texturing parameters have therefore yet to be established for all materials [1–4].

In this work, the multiscale nano- and microtexturing modes were studied for the surfaces of different structural materials subjected to IR femtosecond laser radiation with subsequent hydrophobization using chemisorbed hydrophobic agents, and the key param-

eters of the wettability of the resulting hydrophobized surface textures were determined.

EXPERIMENTAL

A Satsuma ytterbium-doped fiber laser (Amplitude Systems) [7] was used as our ultra-short pulse (USP) source. The radiation of the fundamental laser harmonic at a wavelength of 1030 nm with a half-height duration of around 300 fs and a maximum pulse energy as high as 10 μJ in the TEM₀₀ mode at a pulse-repetition frequency $f = 0\text{--}2$ MHz was focused onto each sample's surface in air through a KI-8 glass lens with $F = 35$ mm onto a spot with radius $R_1 \approx 15$ μm . Our aluminum, titanium, and copper samples were in the form of ~ 1 mm thick plates with surfaces of optical quality, mechanically polished with a 0.15 μm grain paste. The titanium samples were fabricated in the form of half-bars with total diameters of 8 mm. A commercial 3 mm thick plate of optically transparent Plexiglas was used with pretreatment. The samples were placed on a motorized three-axis translation stage with a minimum travel step of 150 nm and scanned by the laser beam at different platform conveying speeds (see Table 1), creating a textured section

Table 1. Parameters of the IR laser texturing of our materials' surfaces

Material	Energy (μJ)	f , kHz	V , mm s ⁻¹	Spacing between lines, μm
Aluminum	6	250	6	24
Titanium no. 1	6	250	6	24
Titanium no. 2	2	250	6	24
Titanium no. 3	2	250	6	24
Copper no. 1	10	250	6	24
Copper no. 2	10	250	6	12
Plexiglas	10	250	6	12

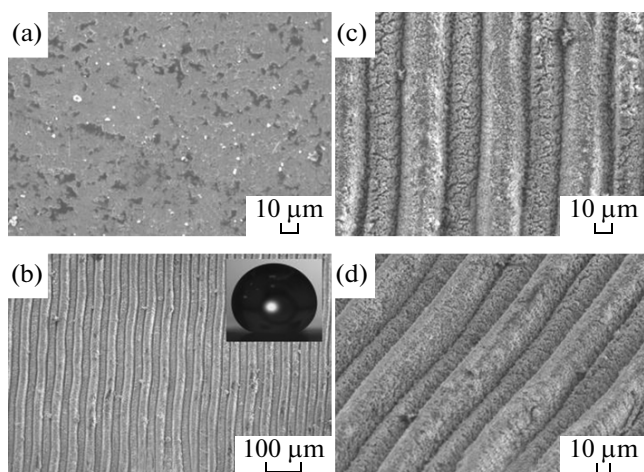


Fig. 1. SEM images of the surface of titanium sample no. 1 (a) before texturing and (b–d) after texturing (at different magnifications; (d) at an angle of 40°). A light microscopy (LM) image of a microdroplet on the texturing is shown in the insert in panel (b).

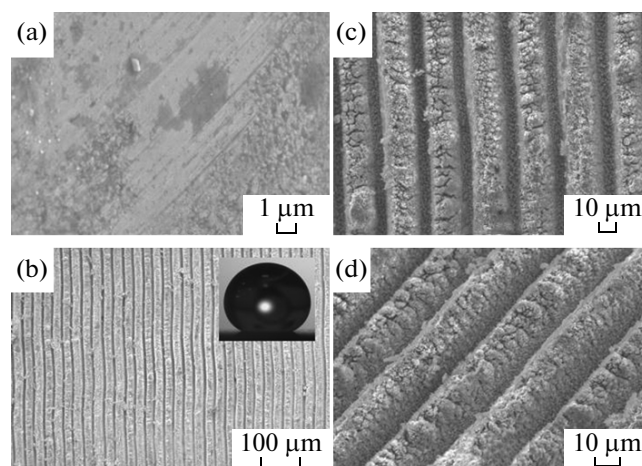


Fig. 2. SEM images of the surface of titanium sample no. 2 (a) before texturing and (b–d) after texturing (at different magnifications; (d) at an angle of 40°). An LM image of a microdroplet on the texturing is shown in the insert in panel (b).

of the sample 1×1 cm in size. The surface geometry was visualized using a JEOL 7001F scanning electron microscope.

The surface textures were hydrophobized via the chemisorption of hydrophobizing agent methoxy- $\{3-[(2,2,3,3,4,4,5,5,6,6,7,7,8,8,8\text{-pentadecafluorooctyl})\text{-oxy}]\text{-propyl}\}$ -silane from a 20% solution in 99% decane (Acros Organics). The samples were immersed into the solution for 2 h and then dried in an oven at 140°C for 60 min [8].

The wettability of the samples with textured and hydrophobized surfaces was studied by measuring the contact and roll-off angles after videotaping the behavior of drops [9, 10]. The contact angles were measured in five different sections of the surfaces; drops with volumes of 10–15 μL were used in our measurements. To measure the roll-off angles, 10 μL drops were placed in ten surface sections. Once the drops assumed equilibrium shape, the sample was inclined in a controllable manner and the roll-off angle of each drop was recorded.

RESULTS AND DISCUSSION

The topographies of the obtained multiscale surface textures are presented in Figs. 1–5 for different materials before they were hydrophobized.

The surface textures of titanium samples 2 and 3, fabricated at low USP energies, are shown in Figs. 1 and 2. For comparison, the plate from sample no. 1 acquired holes as a result of ablation at a higher USP energy of around 6 μJ (Table 1), indicating the moderate reflectance of titanium in the IR range and its low USP ablation threshold [11]. The texturing of different titanium samples under equal conditions yielded

easily reproducible textures (Figs. 1 and 2) and virtually the same contact angles, within the limits of the experimental error (Table 2).

In a similar manner, the texture of copper sample no. 2 (Figs. 3 and 4) with more distinct modulation (Fig. 4) obtained as a result of overlapping the scanning lines at a smaller increment (12 μm against 24 μm; see Table 1) had a higher contact angle after hydrophobization and a somewhat smaller roll-off

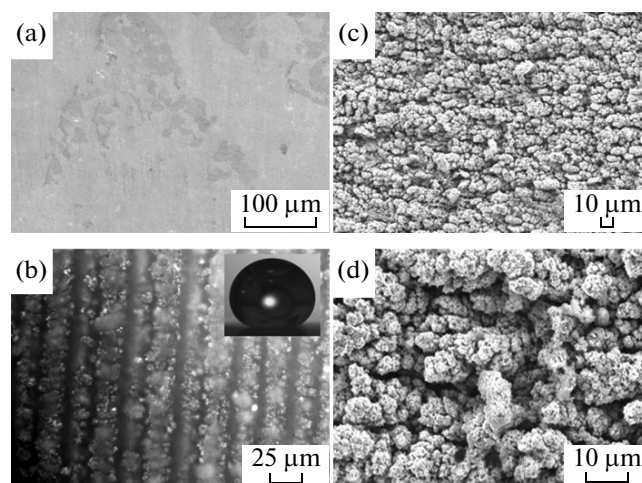


Fig. 3. SEM and LM images of the surface of copper sample no. 2 (a) before texturing and (b–d) after texturing (at different magnifications). The images in panels (c) and (d) show the topography of the texture ridges. An LM image of a microdroplet on the texturing is shown in the insert in panel (b).

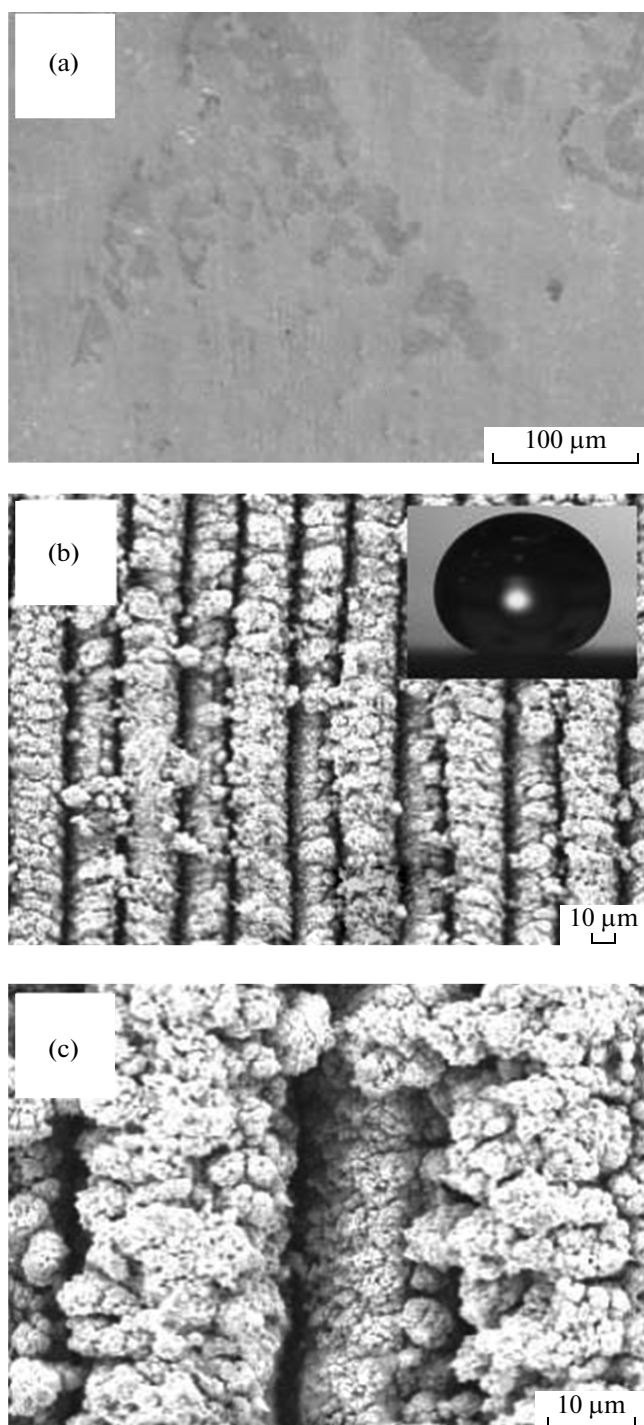


Fig. 4. SEM images of the surface of copper sample no. 3 (a) before texturing and (b–c) after texturing (at different magnifications). An LM image of a microdroplet on the texturing is shown in the insert in panel (b).

angle (Table 2). For comparison, the aluminum sample with an extremely weak texture modulation (Fig. 5)—evidence of the high reflectance of aluminum in the IR range and thus negligible ablation of its

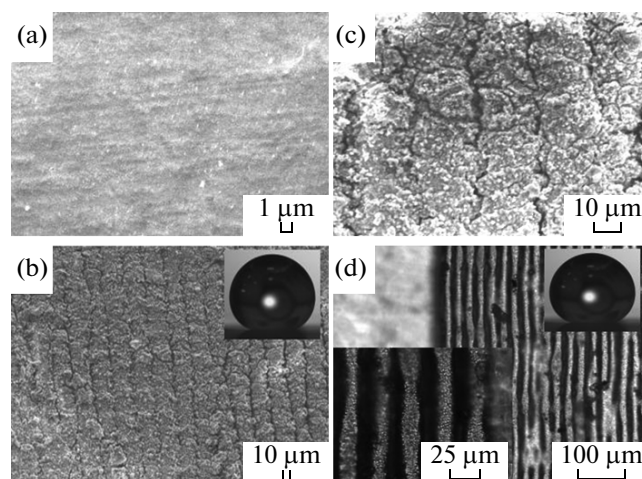


Fig. 5. SEM images of the surface of the aluminum sample (a) before texturing, (b–c) after texturing (at different magnifications), and (d) LM images of the surface of the Plexiglas sample at a different magnification. LM images of microdroplets on the texturing are shown in the inserts in panels (b) and (d).

surface under the conditions of the experiment in question—also had a relatively low contact angle and no drops rolling off (Table 2). In contrast, the Plexiglas sample with strong modulation of the surface texture (Fig. 5d) reveals the superhydrophobic nature of the surface with a high contact angle and a low roll-off angle (Table 2). Interestingly, the laser texturing of the copper, aluminum, and Plexiglas samples required almost the maximum USP energy (energy density) to compensate for the high reflectance of these metals and the high transmissivity of Plexiglas in the IR range [12].

Table 2. Contact angles and roll-off angles of hydrophobized texture surfaces

Material	Contact angle (deg)	Roll-off angle (deg)
Aluminum	141 ± 3	No off-rolling
Titanium no. 2	159 ± 5	11 ± 4
Titanium no. 3	162 ± 3	17 ± 7
Copper no. 1	163 ± 3	23 ± 9
Copper no. 2	166 ± 5	18 ± 7
Plexiglas	160 ± 2	13 ± 4

CONCLUSIONS

Multiscale femtosecond laser texturing of samples of various structural materials by varying the laser pulse energy and the spacing between the scanning lines on the surface allowed us to fabricate on a reproducible basis multimodal textures that ensure the superhydrophobic properties of the materials' surfaces upon hydrophobization. The high modulation amplitude of the surface texture after laser processing allowed us to achieve high contact angles (more than 150° – 160° as a rule) and roll-off angles of less than 20° .

ACKNOWLEDGMENTS

This work was supported by the Presidium of the Russian Academy of Sciences, project no. 24.

REFERENCES

1. Kudryashov, S.I., Kolobov, Yu.R., and Ligachev, A.E., *Fotonika*, 2014, vol. 3, no. 45, p. 14.
2. Ionin, A.A., Kudryashov, S.I., Makarov, S.V., et al., *Appl. Phys. A*, 2012, vol. 107, no. 2, p. 301.
3. Ionin, A.A., Klimachev, Y.M., Kozlov, A.Y., et al., *Appl. Phys. B*, 2013, vol. 111, p. 419.
4. Boinovich, L., Domantovskiy, A., Emelyanenko, A., et al., *ACS Appl. Mater. Interfaces*, 2014, vol. 6, no. 3, p. 2080.
5. Ionin, A.A., Kudryashov, S.I., Seleznev, L.V., et al., *J. Exp. Theor. Phys.*, 2013, vol. 116, no. 3, p. 347.
6. Artyukov, I.A., Zayarnyi, D.A., Ionin, A.A., et al., *JETP Lett.*, 2014, vol. 99, no. 1, p. 51.
7. www.amplitude-systemes.com/satsuma-fiber-laser.html
8. Boinovich, L.B., Emelyanenko, A.M., Korolev, V.V., and Pashinin, A.S., *Langmuir*, 2014, vol. 30, no. 6, p. 1659.
9. Emelyanenko, A.M. and Boinovich, L.B., *Instrum. Exp. Tech.*, 2002, vol. 45, p. 44.
10. Emel'yanenko, A.M. and Boinovich, L.B., *Colloid J.*, 2001, vol. 63, p. 159.
11. Golosov, E.V., Ionin, A.A., Kolobov, Yu.R., et al., *J. Exp. Theor. Phys.*, 2011, vol. 113, no. 1, p. 14.
12. Kudryashov, S.I. and Emel'yanov, V.I., *JETP Lett.*, 2001, vol. 73, p. 666.

Translated by O. Lotova